Microfluidic on-chip fluorescence-activated interface control system

Li Haiwang,[1] N. T. Nguyen,[1] T. N. Wong,[1,a)] and S. L. Ng[2]
[1]*School of Mechanical and Aerospace Engineering, Nanyang Technological University, 639798 Singapore, Singapore*
[2]*School of Mechanical and Aeronautical Engineering, Singapore Polytechnic, 139651 Singapore, Singapore*

(Received 10 July 2010; accepted 18 October 2010; published online 22 November 2010)

A microfluidic dynamic fluorescence-activated interface control system was developed for lab-on-a-chip applications. The system consists of a straight rectangular microchannel, a fluorescence excitation source, a detection sensor, a signal conversion circuit, and a high-voltage feedback system. Aqueous NaCl as conducting fluid and aqueous glycerol as nonconducting fluid were introduced to flow side by side into the straight rectangular microchannel. Fluorescent dye was added to the aqueous NaCl to work as a signal representing the interface position. Automatic control of the liquid interface was achieved by controlling the electroosmotic effect that exists only in the conducting fluid using a high-voltage feedback system. A LABVIEW program was developed to control the output of high-voltage power supply according the actual interface position, and then the interface position is modified as the output of high-voltage power supply. At last, the interface can be moved to the desired position automatically using this feedback system. The results show that the system presented in this paper can control an arbitrary interface location in real time. The effects of viscosity ratio, flow rates, and polarity of electric field were discussed. This technique can be extended to switch the sample flow and droplets automatically. © *2010 American Institute of Physics.* [doi:10.1063/1.3516036]

I. INTRODUCTION

Microsystems such as laboratories on a chip play increasingly an important role in the development of new technologies for analytical chemistry and biomedical diagnosis.[1–6] The flow of two stratified streams in a microchannel is often found in applications such as ion exchange or solvent extraction.[7] The Reynolds number in microfluidic devices is typically less than unity, leading to the dominating laminar flow regime.[8] Molecular diffusion at the laminar interface is the only mode of mass transfer between the two streams.[9] Considering diffusive dispersion, Wu and Nguyen[10] used hydrodynamic focusing to control the width and the position of a liquid stream, and this mode of mass transfer was used for extraction and separation in biological species.[11,12] Biological fluid and aqueous reagent, which pose different physical properties, were used in these applications.[13]

In the past, interface control and flow focusing were realized in an open-loop manner by hydrodynamic or electrokinetic mean. Blankenstein and Larsen[14] utilized hydrodynamic spreading to focus a sample stream. Lee *et al.*[15,16] focused one or multiple sample streams and switched these streams to the desired outlets using different flow rate ratios. The same concept of hydrodynamic spreading was utilized by Abkarian *et al.*[17] to measure the pressure difference in the microchannel by monitoring the interface location; this concept allows the realization of a precise

a)Author to whom correspondence should be addressed. Electronic mail: mtnwong@ntu.edu.sg.

low-pressure manometer in microfluidics. However, the pressure technique relies mainly on the flow rate ratio of two fluids; the flow rate ratio is too high when the fraction of one fluid is large.

In recent years, electroosmosis is another popular controlling method. Compared with the pressure-driven method, electroosmosis has many advantages. For example, electroosmotic flow has a uniform flow velocity profile and no moving parts. In microsystems, surface-to-volume ratio is large; electroosmosis is more efficient than ordinary pressure-driven flow. Besselink *et al.*[18] and Kohlheyer *et al.*[19] used electroosmotic flow (EOF) to control and guide sample streams in a multiflow microfluidic system. Electroosmotic concept allowed a simple chip design, a fast and accurate switching between different flow rates.[20] Electroosmotic phenomena in multiflow configurations have been studied in the past. Gao *et al.*[21] presented a mathematical model to describe a two-fluid electroosmotic pumping technique by assuming a planar interface between the two immiscible fluids. Using electroosmotic effect, the interface position of a pressure-driven two-fluid flow can be accurately controlled.[22,23] Electrokinetic control of multiflow systems also lead to mixing enhancement.[24] However, the electroosmotic flow is unstable when the voltage is too high.

To avoid the problems of pressure-driven and electroosmosis, the combination of hydrodynamic and electroosmosis was used in microsystems.[21,22,25–27] While most of the previous studies concentrated on spreading, focusing, and switching either by pressure-driven or by electroosmosis, all these concepts are based on an open-loop control without feedback. The flow rate ratio or the electric fields have to be manually adjusted. In many applications, a closed-loop control of spreading, focusing, or switching is desirable. For feedback from the controlled variable, a detectable signal from the flow system is needed. Fluorescence detection[28] provides a possible mean to return a feedback signal to the flow-driven mechanisms.

In this paper, closed-loop control of the interface location between the two stratified streams was realized by combining pressure-driven and electroosmotic effects and fluorescence detection. Feedback signal for automatic control of the interface location was achieved by detecting the fluorescent intensity. In order to detect the fluorescent signal, light emitting diode was used as the excitation source. The fluorescent signal was transformed into voltage by a photodiode and digitized by an analog-to-digital converter. The control algorithm was realized digitally in a LABVIEW program that uses the feedback signal from the fluorescent measurement to control the high-voltage source of the EOF flow. The experiments controlled the interface to the desired locations automatically using the above systems. The effects of viscosity ratio, flow rates, and polarity of the electric field to the response time were discussed

II. EXPERIMENT

A. Microchannel

Figure 1 shows the H-shaped microchannel used in the experiments. The adhesive lamination technique[29] was used to fabricate the microchannel. Two polymethylmethacrylate (PMMA) plates (50 mm $\times$ 50 mm) were bonded by a double-sided adhesive tape. First, the two PMMA plates were cut using a CO_2 laser platform. Fluidic access holes and alignment holes were also machined by the same laser into the PMMA substrate. Next, a double-sided adhesive tape (Adhesives Research Inc., Singapore, Arclad 8102 transfer adhesive) was cut to form the intermediate layer with the channel structures. The adhesive layer thickness of 50 μm defines the channel's height. The three layers were positioned with the alignment holes and pressed together for bonding. Using the above method, a microchannel with a cross section of 2 mm $\times$ 50 μm and a length of 2 cm was fabricated. As shown in Fig. 1, two fluids, aqueous sodium chloride (NaCl) solution (q_1) and aqueous glycerol (q_2), were introduced through the inlets by two syringes (5 ml gastight, Hamilton), which is driven by one syringe pump (Cole-Parmer, USA, 74900-05; from 0.2 μl/h to 500 l/h, accuracy of 0.5%). An electric field was applied on the NaCl solution by inserting a pair of platinum electrode at ports A and C. The interface position was represented by the dimensionless ratio α between the width of the NaCl stream and the channel width.

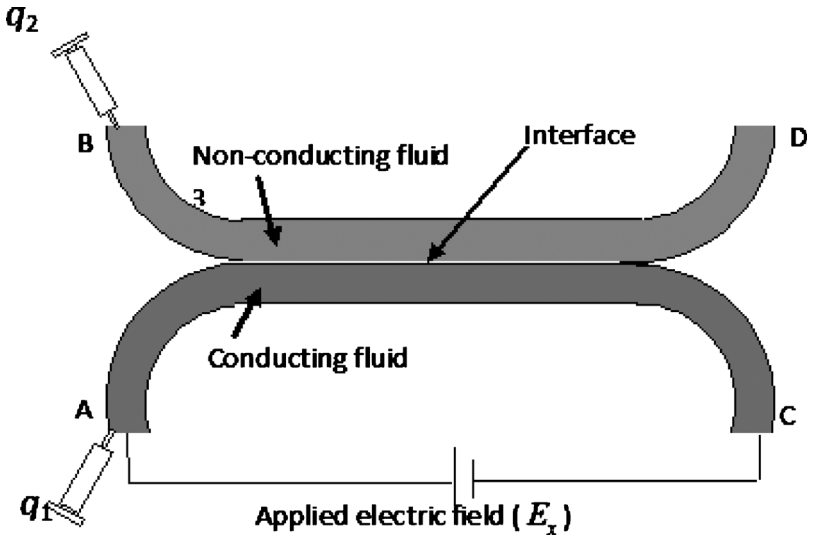

FIG. 1. Schematic representation of the H-shape microchannel.

B. The setup of the control system

A schematic of the experimental setup is shown in Fig. 2. The setup can be used for automatic feedback control of the interface location. The control system consists of four main components: an excitation light source, a signal conversion system, a controlling system, and a high-voltage power supply.

Excitation is done solely by a blue light emitting diode (LED) that has an excitation wavelength centered at 455 nm with a full width at half maximum of about 20 nm. The typical power of this light source is about 220 mW (Laboratory DC Power Supply, Taiwan, GPR-3060D).

The signal conversion system includes four parts: a fluorescent filter (Edmund, United States), a focusing lens (Navitar, USA, 1-61456), a photodiode (Edmund Optics, Barrington, NJ) , and a voltage amplifier (LM358P, STMicroelectronics, Singapore). After being excited, the fluorescence de-ionized (DI) water emits green fluorescence light, which passes though a narrow bandpass interference filter (515 ± 10 nm). The filter is attached to the focusing lens. The filter is used to cut the excitation spectrum of the LED so that it is not interfered by emitting fluorescent signal. The detected optical signal is converted into a voltage by a photodiode. The detected signal is then amplified by an operational amplifier to reach the range from 1 to 10 V; this value is suitable for the data acquisition board.

The control system consists of a data acquisition board with both analog-to-digital and digital-to-analog converters. The detected signal from the photodiode is recorded and displayed by a custom-made LABVIEW program. The detected signal is used as the process variable (the fraction α) for the proportional–integral–differential (PID) control algorithm implemented in the LABVIEW program. The output of the high-voltage power supply (CZE1000R, Spellman, USA) is adjusted automatically by the control system.

C. Experimental setup for imaging

An interline transfer charge-coupled device (CCD) camera (Sony, Japan, ICX 084) was used for recording the images. The CCD camera is attached to the optical system of a Nikon (Japan) inverted

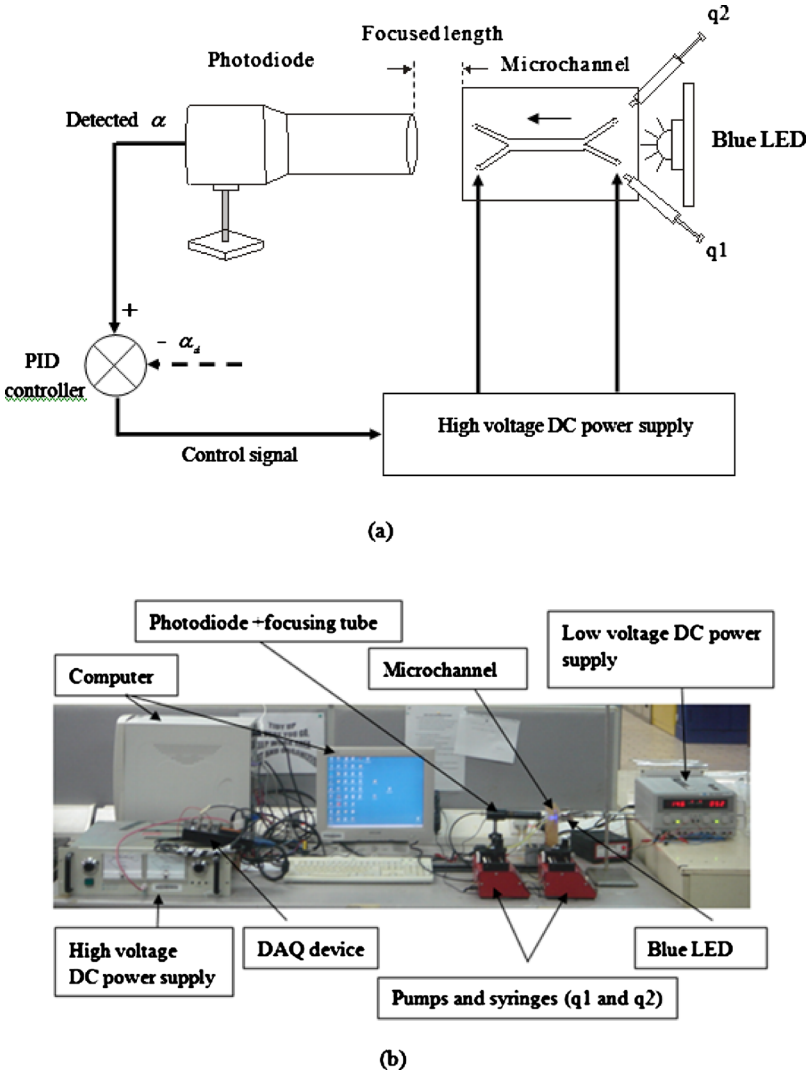

FIG. 2. On-chip fluorescence-activated interface controlling system.

microscope (model ECLIPSE TE2000-S) with a set of epifluorescent attachments. The detail of the experimental setup is the same with that of Li *et al.*[27]

D. Chemical prosperities

NaCl was diluted in DI water with a concentration of $7\times10^{-4}M$; the conductivity and viscosity of the NaCl solution are 86.6 μs/cm and 0.85×10^{-3} N s m^{-2}, respectively. The conductivity and viscosity of the DI water are 0.064 μs/cm and 0.85×10^{-3} N s m^{-2}, respectively. Compared with the aqueous NaCl, the conductivity of the DI water is so low that aqueous NaCl is regarded as conducting fluid and DI water is regarded as nonconducting fluid. The zeta potential at the PMMA channel and NaCl solution is -24.4 mV.[30] The properties of the aqueous glycerol are shown in Tables I–IV.

Fluorescent dye (fluorescein sodium salt $C_{20}H_{10}Na_2O_5$, also called Acid Yellow 73) was added to the aqueous NaCl. The concentration of the fluorescent dye is 0.1 g/l. The excitation wavelength of the fluorescent dye is 460 nm and the emission wavelength is 515 nm.

TABLE I. Fluid conditions and controlled parameters (q_1 is the flow rate of fluid 1; q_2 is the flow rate of fluid 2; β is the viscosity ratio; μ_1 is the dynamic viscosity of fluid 1; μ_2 is the dynamic viscosity of fluid 2; K_c is the proportional gain of the controlled system; T_i is the integral time of the controlled system; T_d is the derivative time of the controlled system; and Δt is the periodic time of the system).

	Fluid	Flow rate (ml/h)	$\beta=\frac{\mu_2}{\mu_1}$	Control action
q_1	Aqueous NaCl($7\times10^{-4}M$, $\mu_1=0.85\times10^{-3}$ N s/m^2) +Acid Yellow 73	0.05	1	$K_c=10$, $T_i=0.008$ min, $T_d=0.001$ min, $\Delta t=1$ s
q_2	DI water	0.1		

TABLE II. Fluid conditions and controlled parameters.

Expt. No.		Fluid	Flow rate (ml/h)	$\beta=\frac{\mu_2}{\mu_1}$	α_i	α_d	Controlaction
1	q_1	Aqueous NaCl+Acid Yellow 73	0.5				
	q_2	DI water	0.05	1	0.8	0.5	$K_c=10$, $T_i=0.008$(min), $T_d=0.001$(min), $\Delta t=1$(s)
2	q_1	Aqueous NaCl+Acid Yellow 73	0.5				
	q_2	Aqueous glycerol (volume concentration 30%, $\mu_2=3.27\times10^{-3}$ N s/m^2)	0.025	3.27	0.8	0.5	

TABLE III. Fluid conditions and controlled parameters.

Expt No		Fluid	Flow rate (ml/h)	$\beta=\frac{\mu_2}{\mu_1}$	α_i	α_d	Control action
1	q_1	Aqueous NaCl+Acid Yellow 73	0.5				
	q_2	Aqueous glycerol (volume concentration 10%, $\mu_2=1.24\times10^{-3}$ Ns/m^2)	0.04	1	0.8	0.5	$K_c=10$, $T_i=0.008$(min), $T_d=0.001$(min), $\Delta t=1$(s)
2	q_1	Aqueous NaCl+Acid Yellow 73	1				
	q_2	Aqueous glycerol (volume concentration 10%,)	0.08	1	0.8	0.5	

TABLE IV. Fluid conditions and controlled parameters.

Case		Fluid	Flow rate (ml/h)	α_i	α_d	e	Control action
(a)	q_1	Aqueous NaCl+Acid Yellow 73	0.5			$\frac{q_1}{q_2}=2$	
	q_2	DI water	0.25	0.7	0.5	0.2	$K_c=10$, $T_i=0.008$(min), $T_d=0.001$(min), $\Delta t=1$(s)
(b)	q_1	Aqueous NaCl+Acid Yellow 73	0.25			$\frac{q_1}{q_2}=\frac{1}{2}$	
	q_2	DI water	0.5	0.3	0.5	0.2	

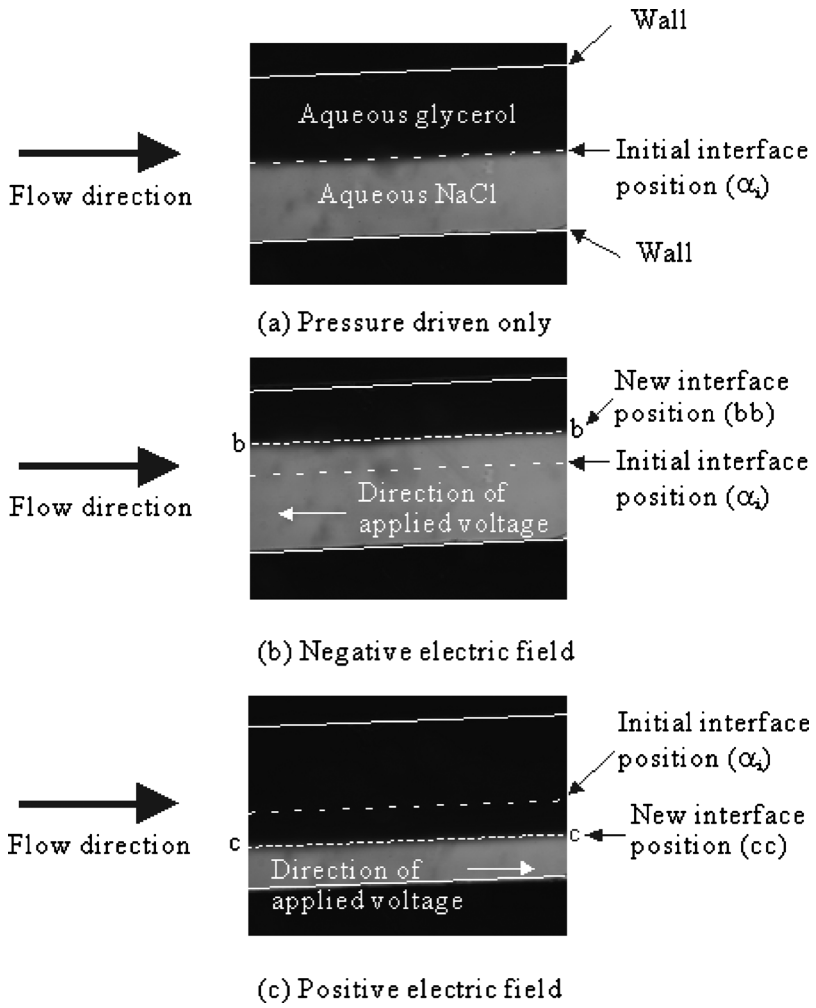

FIG. 3. Concept of the interface position control using the electroosmosis effect.

III. CONCEPT OF CONTROL

A. Effect of electroosmosis

Figure 3 shows the effect of electroosmosis, which is the fundamental effect for our control scheme. When no electric field is applied, the flow is simply driven by a pressure gradient. The interface position is initial interface position, α_i [Fig. 2(a)]. According to Wang *et al.*,[31] the velocity of particle in the conducting fluid can be expressed as

$$u_{\text{particle}} = u_{\text{EOF}} + u_{\text{pressure}} + u_{\text{eph}} + u_b, \tag{1}$$

where u_{EOF} is the velocity of electroosmosis, u_{eph} is the electrophoresis velocity of the particle, u_{pressure} is the velocity of pressure-driven flow, and u_b is the velocity due to Brownian motion of the particle. u_{eph} can be expressed as

$$u_{\text{eph}} = \frac{\varepsilon E_x \xi_p}{\mu}, \tag{2}$$

where ξ_p is the particle's surface zeta potential, and ε and μ are the permittivity and the dynamic viscosity of the fluid, respectively.

Under the effect of negative electric field, the electroosmotic flow acts against the pressure-driven flow; the velocity of the particle is also negative. Consequently, the NaCl solutions encounter a larger resistance. The NaCl solutions appear to be more "viscous" due to the electroosmotic effect. Due to the same pressure drop along the microchannel and the same volumetric flow rate forced by the syringe pump, the more viscous fluid has to spread over a larger area; thus, the interface is pushed to a new position (bb) [Fig. 3(b)]. If positive electric field is applied to the conducting fluid, the electroosmotic flow is in the same direction as the pressure-driven flow, and the velocity of the particle is positive, then the NaCl solutions can flow faster. Under a constant flow rate, the conducting fluid occupies a smaller part of the microchannel and the interface is pulled to another new position (cc) [Fig. 3(c)]. The moving distance of the interface can be controlled by the magnitude of the electric field.[21,22]

B. Concept of the system

Figure 2 shows the process of the system. First, aqueous NaCl and aqueous glycerol are pushed into the microchannel using the syringes. The position of the interface is the initial interface position, α_i. The fluorescent dye in the aqueous NaCl is excited by the blue LED and emits the fluorescent signal (green light). The signal is filtered and focused using a filter a lens. The improved fluorescent signal is detected by the photodiode. The detected signal strength varies according to the relative interface location. A higher fraction of aqueous NaCl, α, emits stronger fluorescent signal. The PID controller compares the desired interface position (α_d) with the detected position (α) and returns a feedback signal in a form of voltage from the dc power supply. Thus, the voltage across the aqueous NaCl stream varies according the control signal. For a constant flow rate, the interface location can be regulated automatically to the desired interface position by the electroosmotic effect.

IV. RESULTS AND DISCUSSION

A. Image point of focused tube

From imaging theory,[32] a positive or converging lens in air can focus the beams emitted from one point and form a real image at the focal point. If the fluorescent image is focused at a spot, the energy of this spot has a maximum value. We assume that the LED is a point source; if the photodiode is positioned at the focal point of the imaging system, it can detect the highest energy.

To determine the focal length, the blue LED is activated and placed in line with the microchannel and the photodiode. Two de-ionized water with the fluorescent dye ($C_{20}H_{12}O_5$) was pumped from the two inlets of the microchannel to ensure a maximum photocurrent. Figure 4 illustrates the photocurrent output and the photodiode location. The results indicate that a maximum signal is observed when the photodiode reach a focal length of approximately 370 mm. The photosensor is kept at this position for all subsequent experiments.

B. The relationship between the fluorescence signal and the fraction of the aqueous NaCl

In this part, aqueous NaCl and DI water are used in the experiment. The liquid fraction of aqueous NaCl is defined as

$$\alpha = \frac{h_1}{H}, \tag{3}$$

where H is the width of the microchannel, $H=h_1+h_2$; h_1 and h_2 are the heights of aqueous NaCl and aqueous glycerol, respectively.

Three steps are proceeded to find the relationship between the fluorescence and the fraction of the aqueous NaCl. First, the relationship between the interface position and the flow rate ratio is obtained. The fluorescent image is recorded by an epifluorescent attachment of type Nikon G-2E/C. The interface positions are determined using the recorded images and a customized image

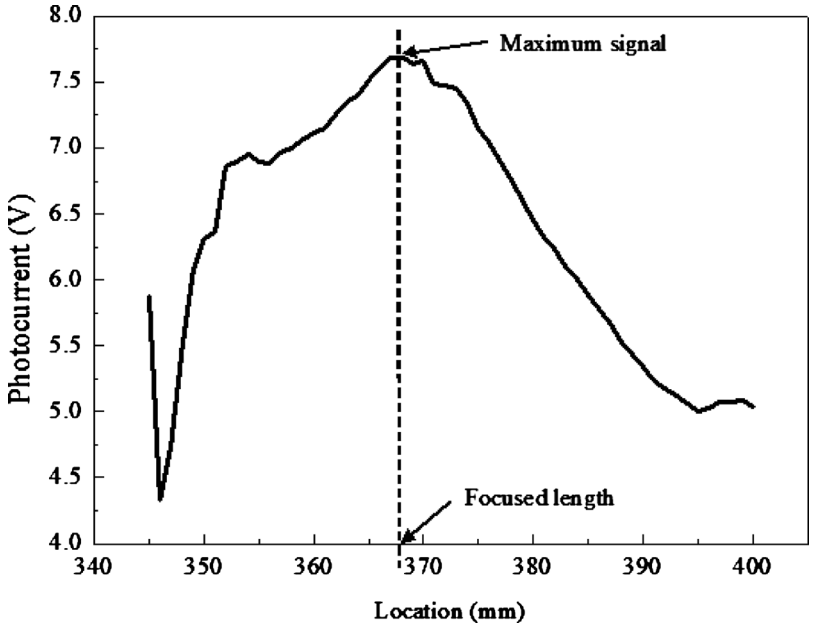

FIG. 4. Determination of the focused length.

processing program written in MATLAB.[29] Because of the mixing effect, an interdiffusion region exists at the interface. This paper assumes that the inner diffusion of dye between the two fluids is a Gaussian distribution. A MATLAB program is developed to determine the interface position. The program calculates the position (y) basing on the derivative of concentration c with respect to the distance, y, which can be taken by the formula $(c_2-c_1)/(y_2-y_1)$. The interface position is taken as the position where dc/dy has its maximum value. Figure 5(a) shows the relationship between the flow rate ratio and the interface position. Aqueous NaCl and DI water are used in the experiment.

Second, determine the relationship between the fluorescent signal and the flow rate ratio. The dimensionless fluorescent signal from the photodiode is defined as

$$I^* = \frac{I - I_{\min}}{I_{\max} - I_{\min}}, \tag{4}$$

where I is the actual fluorescent signal, $I_{\max}$ is determined when aqueous NaCl occupies the whole microchannel ($h_1=H$; $\alpha=1$), and $I_{\min}$ is determined when aqueous glycerol occupies the whole microchannel ($h_1=0$; $\alpha=0$). The fluorescent signal I^* for different flow rate ratios is shown in Fig. 5(a).

According to the results of the first and second parts, the relationship between the fluorescence and the fraction of the aqueous NaCl can be obtained. The fluorescent signal I^* for different fractions of aqueous NaCl(α) is shown in Fig. 5(b). The results show that the fluorescent signal I^* is linearly proportional to α.

C. Electroosmotic controller

Figure 6 shows the response curve of the system subjected to multiple steps inputs. Flow conditions and controlled parameters are shown in Table I. One can observe that if the values of K_c, T_i, and T_d are chosen properly, a quick response with small oscillation can be achieved. When the desired interface position (α_d) is adjusted from 50% to 39% and from 39% to 61%, the PID algorithm gives a stable response, and the liquid interface location approaches the desired interface position α_d smoothly and quickly.

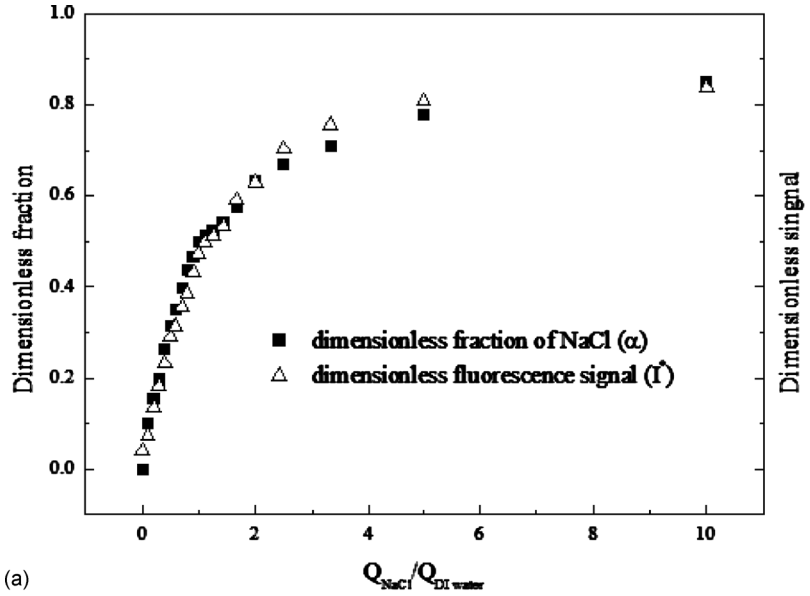

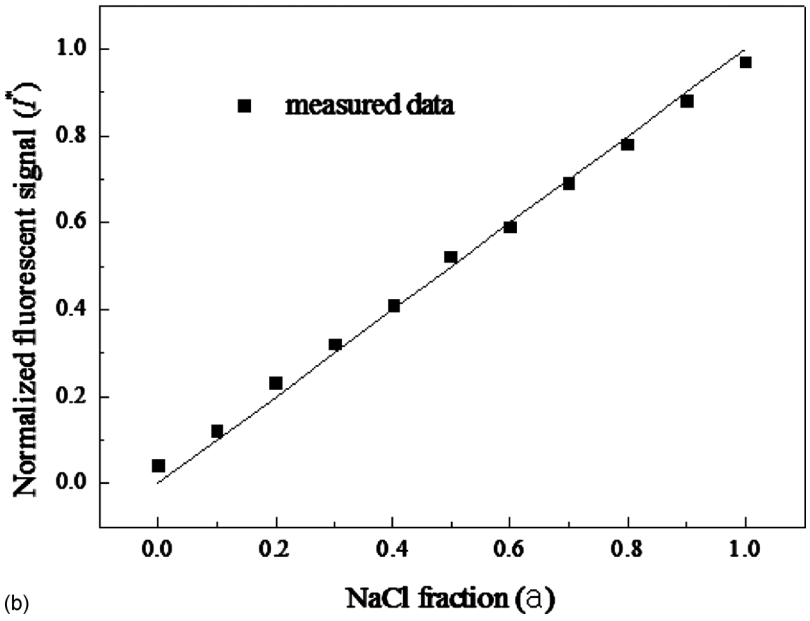

FIG. 5. (a) The relationship between the flow rate ratio and the dimensionless fluorescent signal (the liquid fraction of aqueous NaCl). (b) The relationship between the dimensionless fluorescent signal and the liquid fraction of aqueous NaCl.

We defined the time from the initial interface position (α_i) to the desired interface position (α_d) as setting time, t_s. A short setting time corresponds to a quick response of the system. The following three parameters that affect the setting time are studied: viscosity ratio, flow rate, and applied electric field.

The results show that the interface can be moved to the desired interface position within 5 s. When the interface reached the desired position, the interface is kept around the desired position until the desired position is changed. The perturbation of the interface at the desired position is lower than 5%.

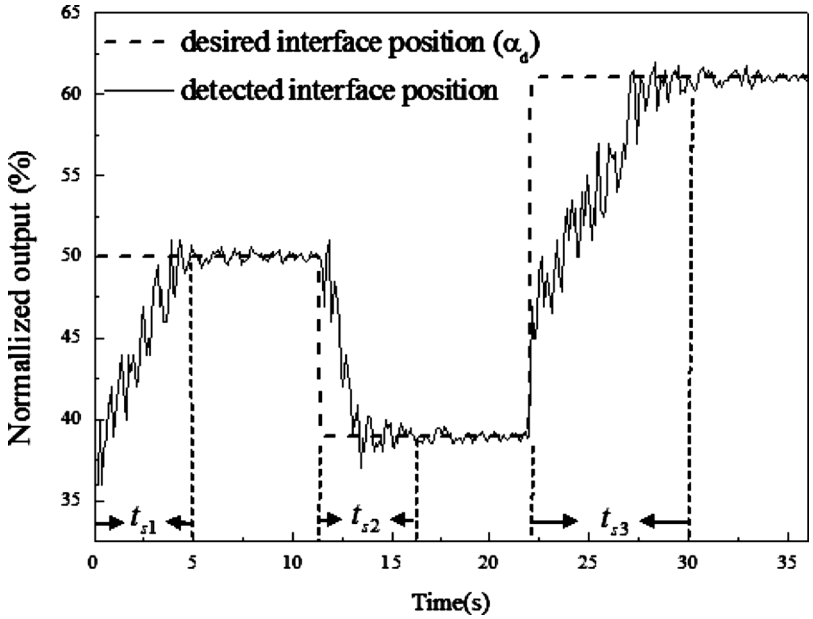

FIG. 6. Response curve of the interface position subjected to multiple step inputs.

D. Effect of viscosity on electroosmotic controller

Figure 7 compares the transient response with different viscosity ratios, $\beta=\mu_2/\mu_1$. The corresponding flow conditions and control parameters are shown in Table II. The transient response of the flow depends on the initial liquid fraction of NaCl, α_i. It is beneficial to maintain the initial liquid fraction of NaCl, α_i, at the same value for comparing the transient response (Table II). Figure 7 shows the transient response of the control system exhibiting a damped oscillation

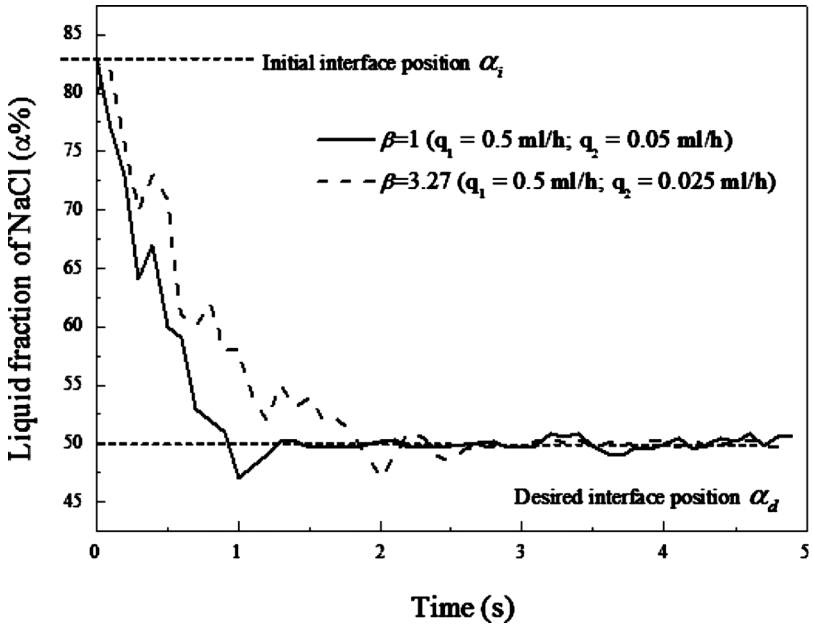

FIG. 7. Response curves of the interface controller for different viscosities.

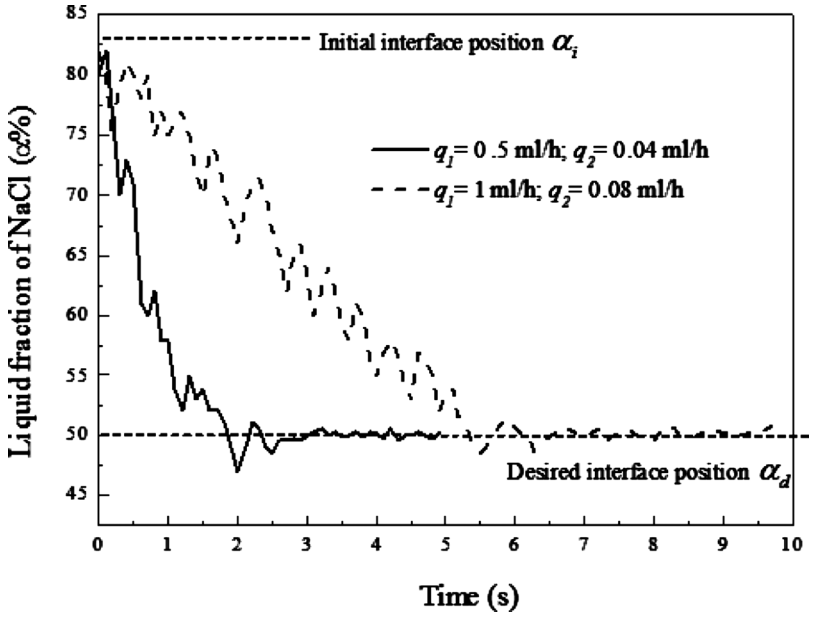

FIG. 8. Response curves of the interface controller for different flow rates.

behavior before reaching the desired interface position (α_d=0.5). The results indicate that the setting time is strongly dependent on the viscosity ratio. The setting time is shorter if the viscosity ratio decreases.

When the viscosity ratio is small, under the condition of constant viscosity of the aqueous NaCl, the flow resistance of the aqueous glycerol is relatively weak. When the electric field changes, the velocity of the aqueous NaCl also changes accordingly. The aqueous glycerol can be driven with less flow resistance and it is more sensitive to the change of the electric field. When the viscosity of the aqueous NaCl increases, the flow resistance of the aqueous glycerol is higher. Under the same change of the electric field, the aqueous glycerol can be driven with more flow resistance and it is less sensitive to the change of the electric field.

E. Effect of flow rate on electroosmotic controller

Figure 8 shows the response curves for different flow rates. The flow conditions and control parameters are shown in Table III. Initially, α_i is maintained at 0.8 as the volumetric flow rate ratio between the two fluids is kept unchanged. Figure 8 indicates that the setting time t_s of a higher flow rate is larger than that of a lower flow rate. A damped oscillation was observed before reaching the desired interface position (α_d=0.5).

The pressure gradient depends on the flow rates of the two fluids. Under high flow rates, where the pressure gradient is higher, larger applied electric fields are required to control the interface position.[23] When the flow rate is high, the velocity of pressure-driven flow is higher. The inertia of the fluid increases. Under the same electroosmosis effect, the velocity is more difficult to be changed when the inertia is higher. Hence, the system is less sensitive to the change of the electric field at higher flow rates. When the flow rate is low, the velocity of pressure-driven flow is lower. The inertia of the fluid decreases. Under the same electroosmosis effect, the velocity is easier to be changed when the inertia is lower. Hence, the system is more sensitive to the change of the electric field at lower flow rates. The results show that setting time is shorter as the flow rates decrease.

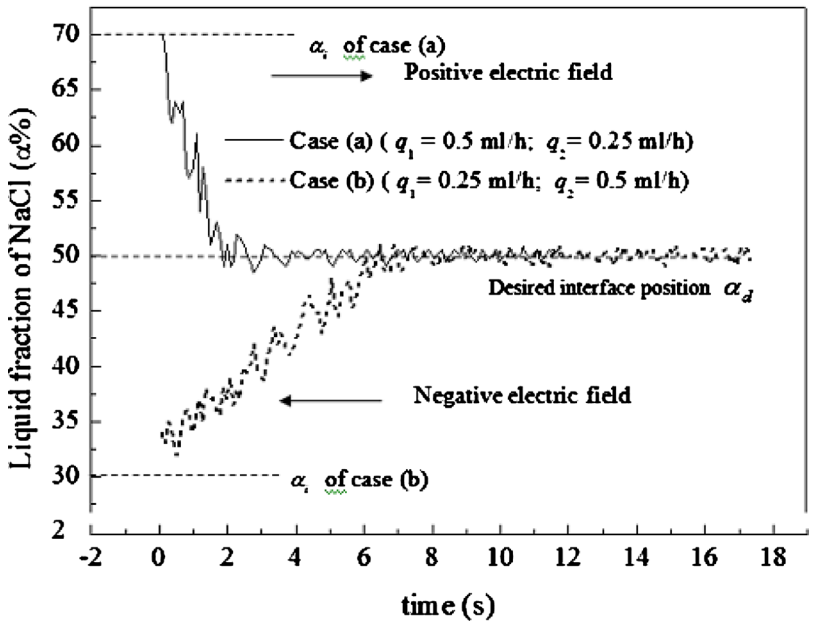

FIG. 9. Response curves of the interface controller for different electric field polarities.

F. The effect of electric field polarity on electroosmotic controller

Figure 9 shows the response curves for different polarities of the applied electric fields. With the flow conditions shown in Table IV, the fraction α_i is maintained at 0.7 and 0.3 for case (a) and case (b), respectively. For a desired interface position of α_d=0.5, both cases result in an error of e=0.2. These results indicate that the setting time t_s is strongly dependent on the polarity of the applied electric field. The setting time is longer if the electric field is negative.

In case (a) with α_i=0.7, aqueous NaCl flows faster as the electroosmotic force acts in the same direction as the pressure-driven flow. According to Eq. (1), the directions of u_{EOF}, u_{eph}, and u_{pressure} are the same. The effect of the electric field on the pressure-driven flow is positive. The NaCl solutions appear to be less viscous due to the electroosmotic effect and the electrophoresis effect. The flow with weaker flow resistance responds to the electric field more quickly.

In case (b) with α_i=0.3, the electroosmotic flow is against the pressure-driven flow when a negative electric field is applied. According to Eq. (1), the directions of u_{EOF} and u_{eph} are opposite to that of u_{pressure}. The effect of the electric field on the pressure-driven flow is negative. The NaCl solutions appear to be more viscous due to the electroosmotic effect and the electrophoresis effect. The flow with stronger flow resistance responds to the electric field slowly.

V. CONCLUSIONS

This paper presents a microfluidic fluorescence-activated interface control system for lab-on-a-chip applications. A LABVIEW program was developed for automatic real-time PID control of the interface. By applying electric field along the conducting liquid, the electroosmotic effect retards or adds the velocity of the conducting fluid, adjusting the interface position. The results indicate that the interface can be moved to the desired position automatically within 5s; when the interface reached the desired position, the interface is kept around the desired position until the desired position is changed. The setting time decreases with a decrease of the flow rates and viscosity ratio and is dependent on the polarity of the applied electric field. Interface control-based microfluidic

devices, such as the T-sensor® and the H-filter®, have been developed for commercial use by Micronics, Inc. (http://www.micronics.net/technologies). The patent of the interface controller has been applied by Wong *et al.*[33] This technique can be extended to switch an optofluidic waveguide.[1–3]

ACKNOWLEDGMENTS

The authors would like to thank the final year project students from the Nanyang Technological University and the Singapore Polytechnic in supporting the experimental work.

[1] H. C. Chang, Biomicrofluidics **3**, 010901 (2009).
[2] S. H. Chang, Biomicrofluidics, **3**, 012802 (2009).
[3] T. Das and S. Chakraborty, Sadhana Acad. Proc. Eng. Sci. **34**, 573 (2009).
[4] F. Sapuppo, A. Llobera, F. Schembri, M. Intaglietta, V. J. Cadarso, and M. Bucolo, Biomicrofluidics **4**, 024108 (2010).
[5] N.-T. Nguyen, Biomicrofluidics **4**, 031501 (2010).
[6] S. Lee, H. J. Park, J. S. Yoon, and K. H. Kanga, Biomicrofluidics **4**, 034102 (2010).
[7] P. Kuban, P. K. Dasgupta, and K. A. Morris, Anal. Chem. **74**, 5667 (2002).
[8] N.-T. Nguyen, *Fundamentals and Applications of Microfluidics* (Artech House, Boston, 2006).
[9] B. H. Weigl, R. L. Bardell, N. Kesler, and C. J. Morris, Anal. Bioanal. Chem. **371**, 97 (2001).
[10] Z. Wu and N. T. Nguyen, Sens. Actuators B **107**, 965 (2005).
[11] H. Hisamoto, T. Horiuchi, M. Tokeshi, A. Hibara, and T. Kitamori, Anal. Chem. **73**, 1382 (2001).
[12] R. B. Dasher, Int. J. Technol. Manage. **23**, 788 (2002).
[13] A. Hatch, E. Garcia, and P. Yager, Proc. IEEE **92**, 126 (2004).
[14] G. Blankenstein and U. D. Larsen, Biosens. Bioelectron. **13**, 427 (1998).
[15] G. B. Lee, C. I. Hung, B. J. Ke, G. R. Huang, and B. H. Hwei, J. Micromech. Microeng. **11**, 567 (2001).
[16] G. B. Lee, B. H. Hwei, and G. R. Huang, J. Micromech. Microeng. **11**, 654 (2001).
[17] M. Abkarian, M. Faivre, and H. A. Stone, Proc. Natl. Acad. Sci. U.S.A. **103**, 538 (2006).
[18] G. A. J. Besselink, P. Vulto, R. G. H. Lammertink, S. Schlautmann, A. van den Berg, W. Olthuis, G. H. M. Engbers, and R. B. M. Schasfoort, Electrophoresis **25**, 3705 (2004).
[19] D. Kohlheyer, G. A. J. Besselink, R. G. H. Lammertink, S. Schlautmann, S. Unnikrishnan, and R. B. M. Schasfoort, Microfluid. Nanofluid. **1**, 242 (2005).
[20] D. Kohlheyer, S. Unnikrishnan, G. A. J. Besselink, S. Schlautmann, and R. B. M. Schasfoort, Microfluid. Nanofluid. **4**, 557 (2008).
[21] Y. Gao, T. N. Wong, C. Yang, and K. T. Ooi, J. Colloid Interface Sci. **284**, 306 (2005).
[22] C. Wang, N. T. Nguyen, T. N. Wong, Z. Wu, C. Yang, and K. T. Ooi, Sens. Actuators, A **133**, 323 (2007).
[23] Y. Gao, C. Wang, T. N. Wong, C. Yang, N. T. Nguyen, and K. T. Ooi, J. Micromech. Microeng. **17**, 358 (2007).
[24] Y. J. Pan, C. M. Ren, and R. J. Yang, J. Micromech. Microeng. **17**, 820 (2007).
[25] Y. Gao, T. N. Wong, C. Yang, and T. O. Kim, Colloids Surf., A **266**, 117 (2005).
[26] Y. Gao, Y. F. Yap, T. N. Wong, J. C. Chai, C. Yang, and K. T. Ooi, Proceedings of the Third International Conference on Microchannels and Minichannels, 2005, pp. 343–348.
[27] H. Li, T. N. Wong, and N. T. Nguyen, Microfluid. Nanofluid. **7** (4), 1 (2009).
[28] R. Irawan, C. M. Tay, S. C. Tjin, and C. Y. Fu, Lab Chip **6** (8), 1095 (2006).
[29] Z. Wu, N. T. Nguyen, and X. Huang, J. Micromech. Microeng. **14**, 604 (2004).
[30] D. Yan, N. T. Nguyen, C. Yang, and X. Huang, J. Chem. Phys. **124**, 021103 (2006).
[31] C. Wang, Y. Gao, N. T. Nguyen, T. N. Wong, C. Yang, and K. T. Ooi, J. Micromech. Microeng. **15**, 2289 (2005).
[32] M. J. Kidger, *Fundamental Optical Design* (SPIE, Bellingham, WA, 2002).
[33] T. N. Wong *et al.*, U.S. Patent No. 7,534,0972B2 (19 May 2009).